Dilepton production from the color glass condensate

François Gelis

Laboratoire de Physique Théorique, Bâtiment 210, Université Paris XI, 91405 Orsay Cedex, France

Jamal Jalilian-Marian

Physics Department, Brookhaven National Laboratory, Upton, New York 11973

We consider dilepton production in high energy proton-nucleus (and very forward nucleus-nucleus) collisions. Treating the target nucleus as a color glass condensate and describing the projectile proton (nucleus) as a collection of quarks and gluons as in the parton model, we calculate the differential cross section for dilepton production in quark-nucleus scattering and show that it is very sensitive to the saturation scale characterizing the target nucleus.

I. INTRODUCTION

Perturbative QCD predicts a sharp rise in the number of gluons per unit area and rapidity in a proton or nucleus at high energy (small x) [1]. This however would lead to the violation of unitarity of hadronic cross sections at high energies. High gluon density and gluon recombination effects [2] are believed to be responsible for taming this growth and restoration of unitarity. It has been suggested that gluons at small x can be described by a strong classical field [3] and that weak coupling, semiclassical methods can be applied to describe the physics of dense gluonic systems, such as a proton or nucleus at high energies. This dense system of gluons (the color glass condensate) is characterized by a saturation momentum $Q_s(x)$ which grows fast with energy and rapidity.

There has been much work done in order to investigate the properties of the color glass condensate in deep inelastic electron-proton and electron-nucleus scattering (DIS), as well as proton-nucleus and nucleus-nucleus collisions [4]. While the saturation effects in protons at current energies are far from being established [5], the situation in high energy nucleus-nucleus collisions is more intriguing. The saturation model seems to work reasonably well at the BNL Relativistic Heavy Ion Collider (RHIC) [6] even though there are a lot of open questions which need to be addressed before one can claim that the saturation model describes high energy heavy ion collisions at RHIC quantitatively. The role of final state interactions, thermalization, etc., is still to be understood [7].

In a recent set of publications [8,9], we proposed that high energy proton-nucleus collisions at forward rapidities at RHIC may be an ideal place in order to investigate the color glass condensate and the saturation model. By considering proton-nucleus collisions in the forward rapidity region, one can avoid most, if not all, of the complications present in a nucleus-nucleus collision. Previously, we calculated (real) photon production rate in $p-A$ collisions [9] and showed that it is very sensitive to saturation effects in the nucleus.

In this work, we consider dilepton (virtual photon) production in $p-A$ and show that dileptons provide a more versatile probe of the saturation model than photons. Furthermore, photons are notoriously difficult to measure in a col-

lider environment. One needs to define isolation criteria in order to separate photons from different sources which greatly reduces the production rates in addition to introducing theoretical ambiguities in defining the isolation criteria. The use of factorization theorems, well established for high $p_\perp$ *inclusive* photon production, may be questionable for isolated photons. By considering dilepton production, one can avoid most of these experimental and theoretical difficulties [11].

We briefly review our formalism and the differences between real and virtual photon cross sections in Sec. II. In Sec. III, we consider the diffractive cross section and show that it vanishes. We consider the inclusive cross section in Sec. IV and derive the differential cross section for dilepton production in $p-A$ collisions $d\sigma/dz\, dM^2\, d^2\bm{k}_\perp$, where M^2 and $\bm{k}_\perp$ are the dilepton invariant mass and transverse momentum while z is its fractional energy. We end by discussing our results and the experimental signatures of saturation effects.

II. REAL VS VIRTUAL PHOTON PRODUCTION

In order to reuse some parts of the calculation we already performed for real photon production [9], we start by a section highlighting the main differences between real photon and lepton pair production, as well as the common aspects.

We want to calculate the amplitude for the elementary process

$$q(\bm{p})+A\rightarrow q(\bm{q})+l^+(\bm{k}_1)+l^-(\bm{k}_2)+X \qquad (1)$$

where a quark entering in the color field of a nucleus emits a lepton pair l^+l^-. In terms of *in* and *out* states, this amplitude reads

$$
\begin{aligned}
&\langle q(\bm{q})l^+(\bm{k}_1)l^-(\bm{k}_2)_{\text{out}}|q(\bm{p})_{\text{in}}\rangle \\
&\quad =\langle 0_{\text{out}}|b_{\text{out}}(\bm{q})b_{\text{in}}^\dagger(\bm{p})c_{\text{out}}(\bm{k}_2)d_{\text{out}}(\bm{k}_1)|0_{\text{in}}\rangle, \quad (2)
\end{aligned}
$$

where $b^\dagger$ is the creation operator for a quark, while $c^\dagger$ and $d^\dagger$ respectively create a lepton and an antilepton. Applying the
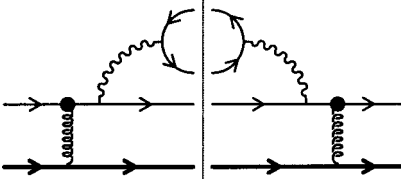
FIG. 1. A typical contribution to the cross section for lepton pair production in pA collisions. The black dot denotes the resummed interactions of the incoming quark with the classical color field of the nucleus. This is the square of the term where the photon is emitted after the scattering on the nucleus. There is also a term where the photon is emitted first, and interferences thereof, not represented here.

LSZ reduction formula to this amplitude [12], one obtains the following expression in terms of the fermionic fields:

$$\langle 0_{\text{out}}|b_{\text{out}}(\boldsymbol{q})b_{\text{in}}^{\dagger}(\boldsymbol{p})c_{\text{out}}(\boldsymbol{k}_2)d_{\text{out}}(\boldsymbol{k}_1)|0_{\text{in}}\rangle$$

$$= \int d^4x\, d^4y\, d^4z_1\, d^4z_2 e^{i(q\cdot x - p\cdot y)}\, e^{i(k_1\cdot z_1 + k_2\cdot z_2)}\bar{u}(\boldsymbol{q})$$

$$\times \bar{w}(\boldsymbol{k}_2)(i\overrightarrow{\partial}_x - m)(i\overrightarrow{\partial}_{z_2} - m)$$

$$\times \langle 0_{\text{out}}|T\psi(x)\bar{\psi}(y)\bar{\Psi}(z_1)\Psi(z_2)|0_{\text{in}}\rangle$$

$$\times (i\overleftarrow{\partial}_y + m)(i\overleftarrow{\partial}_{z_1} + m)v(\boldsymbol{k}_1)u(\boldsymbol{p}), \quad (3)$$

where ψ is the quark field, Ψ the leptonic field, u a quark free spinor, w a lepton free spinor and v an antilepton free spinor. Note that we have approximated all the renormalization constants by 1 since we are going to compute only the lowest order in the couplings α_{em} and α_s. Therefore this amplitude is made of a quark line and a leptonic line, connected by photons. The quark line interacts with the background color which is used to describe the high energy nucleus. At lowest order in the electromagnetic and strong coupling constants, only one bare photon connects the two fermionic lines, as illustrated in Fig. 1.

The part of the diagram that describes the scattering of the quark in the color field of the nucleus is identical to what we have already calculated for the case of photon production. Namely, the photon can be attached before or after the scatterings, but the terms where the photon is attached between scatterings of the quark on the nucleus are suppressed by inverse powers of the center of mass energy $\sqrt{s}$. Therefore, compared to the photon production case, we need only to replace the photon polarization vectors of the produced photon by the propagator of the (now virtual) photon, its coupling to the leptonic line and the spinors of the l^+l^- pair. This amounts to the following substitution:[1]

---

[1]We have indicated the $i\epsilon$ prescription for the photon propagator, but it is in fact irrelevant here since the photon must have an invariant mass squared k^2 larger than $4m_l^2$ because of the threshold for the production of a pair of leptons with mass m_l.

$$\epsilon_{\mu}(\boldsymbol{k})\epsilon_{\nu}^*(\boldsymbol{k}) \rightarrow \frac{g_{\mu\rho}}{k^2 + i\epsilon}\frac{g_{\nu\sigma}}{k^2 - i\epsilon}L^{\rho\sigma}(k_1, k_2), \quad (4)$$

where $k \equiv k_1 + k_2$ is the 4-momentum of the virtual photon, and where $L^{\rho\sigma}(k)$ is the discontinuity of the one-loop leptonic contribution to the photon polarization tensor (i.e. the loop on the upper part of the diagram of Fig. 1—only its discontinuity is needed since the leptons are produced on-shell).

An important simplification we used in the photon case was that the sum over the photon polarizations turned the product $\epsilon_{\mu}(\boldsymbol{k})\epsilon_{\nu}^*(\boldsymbol{k})$ into $-g_{\mu\nu}$ (up to terms proportional to k_{μ} that do not contribute thanks to Ward identities). This property led to a dramatic simplification of the Dirac algebra involved in the calculation of the photon production cross section. A priori, the object $L^{\rho\sigma}(k_1, k_2)$ is not proportional to $g^{\rho\sigma}$, which means that the *fully differential* lepton pair production cross section has a more complicated Lorenz structure. If however we assume that one reconstructs the virtual photon 4-momentum from the momenta k_1, k_2 of the components of the lepton pair, the same simplification occurs. Indeed, if one integrates over the lepton momentum inside the leptonic tensor $L^{\rho\sigma}$, keeping the sum $k = k_1 + k_2$ fixed, we obtain the following result:

$$L^{\rho\sigma} = \frac{2}{3}\alpha_{\text{em}}(g^{\rho\sigma}k^2 - k^{\rho}k^{\sigma}). \quad (5)$$

Therefore, for the cross section $d\sigma/d^4k$, we have the same simplification as in the photon production case.

The relation between the differential cross section and the amplitude can therefore be written as

$$d\sigma = \frac{d^4k}{(2\pi)^4}\frac{d^3\boldsymbol{q}}{(2\pi)^3 2q_0}\frac{1}{2p^-}\frac{2\alpha_{\text{em}}}{3k^2}\mathcal{M}^{\mu}(\boldsymbol{p}|\boldsymbol{q}k)\mathcal{M}_{\mu}^*(\boldsymbol{p}|\boldsymbol{q}k)$$

$$\times 2\pi\delta(q^- + k^- - p^-), \quad (6)$$

where $\mathcal{M}^{\mu}$ is the amplitude for the production of a virtual photon, amputated of its external legs, and from which the factor $2\pi\delta(q^- + k^- - p^-)$ has been removed. Explicitly, we have

$$\mathcal{M}^{\mu}(\boldsymbol{p}|\boldsymbol{q}k) = -ie_q\bar{u}(\boldsymbol{q})\left[\frac{\gamma^-(\not{p} - \not{k} + m)\gamma^{\mu}}{(p - k)^2 - m^2}\right.$$

$$\left. + \frac{\gamma^{\mu}(\not{q} + \not{k} + m)\gamma^-}{(q + k)^2 - m^2}\right]u(\boldsymbol{p})$$

$$\times \int d^2\boldsymbol{x}_{\perp}e^{i(\boldsymbol{q}_{\perp} + \boldsymbol{k}_{\perp} - \boldsymbol{p}_{\perp})\cdot\boldsymbol{x}_{\perp}}(U(\boldsymbol{x}_{\perp}) - 1), \quad (7)$$

where e_q is the electrical charge of the quark and where $U(\boldsymbol{x}_{\perp})$ is a matrix in the fundamental representation of $SU(N_c)$ that represents the interactions of the quark with the classical color field of the nucleus:

$$U(\boldsymbol{x}_{\perp}) \equiv T\exp\left\{-ig^2\int_{-\infty}^{+\infty}dz^-\frac{1}{\nabla_{\perp}^2}\rho_a(z^-, \boldsymbol{z}_{\perp})t^a\right\} \quad (8)$$

with t^a in the fundamental representation, and where $\rho_a(z^-, \mathbf{z}_\perp)$ is the density of color sources in the nucleus. The color averages over the distribution of hard color sources in the nucleus are identical to the case of photon production, and can be found in Sec. III of [9].

The factor $\mathcal{M}^\mu \mathcal{M}^*_\mu$ in the cross section differs from the factor we denoted $|\mathcal{M}|^2$ in our calculation of photon production only in the fact that we must not assume $k^2 = 0$ in the calculation. In fact, in this quantity, only the factor $\langle \mathrm{tr}(L^\dagger L) \rangle_{\mathrm{spin}}$ that contains the Dirac algebra is affected by this change. Its new value is now:

$$
\langle \mathrm{tr}(L^\dagger L) \rangle_{\mathrm{spin}} = 16m^2 \left[\frac{p^{-2}}{D_q^2} + \frac{q^{-2}}{D_p^2} - \frac{k^{-2}}{D_p D_q} \right]
$$

$$
+ 8(p^{-2} + q^{-2}) \left[\frac{2p \cdot q}{D_p D_q} - \frac{1}{D_p} - \frac{1}{D_q} \right]
$$

$$
+ 8k^2 \left[\frac{p^{-2}}{D_q^2} + \frac{q^{-2}}{D_p^2} + \frac{(p^- + q^-)^2}{D_p D_q} \right], \quad (9)
$$

where m is the mass of the quark and where we denote $D_p \equiv (p-k)^2 - m^2 = -2p \cdot k + k^2$ and $D_q \equiv (q+k)^2 - m^2 = 2q \cdot k + k^2$. It is trivial to check that it reduces to the value found in [9] if we set $k^2 = 0$. Having in mind the fact that the quark comes from the wave function of a proton, we neglect the mass of the quark in the following.

III. DIFFRACTION

Like in [9], we can first study the case of diffractive dilepton production, as the kinematics is simpler. Let us just remember that the diffractive cross section is obtained by performing the average over the distribution of nuclear color sources before squaring the amplitude. This implies that no net transverse momentum is exchanged between the nucleus and the quark, i.e. $\mathbf{p}_\perp = \mathbf{q}_\perp + \mathbf{k}_\perp$. If one evaluates the factor $\langle \mathrm{tr}(L^\dagger L) \rangle_{\mathrm{spin}}$ with this kinematical constraint, one obtains a vanishing result if we neglect the mass m of the quark:

$$
\langle \mathrm{tr}(L^\dagger L) \rangle_{\mathrm{spin}}^{\mathrm{diff}} = 0. \quad (10)
$$

This is in fact similar to the case of real photon production: the absence of transverse momentum exchange between the quark and the nucleus prevents the emission of the virtual photon.

IV. INCLUSIVE CROSS SECTION

If we do not require a diffractive process on the nuclear side, we just have to perform the average over colors sources after squaring the amplitude. The details of this procedure are given in Sec. IV of [9]. We obtain the following expression for the differential cross section:

$$
d\sigma_{\mathrm{incl}} = \frac{d^4k}{(2\pi)^4} d^3 \frac{\mathbf{q}}{(2\pi)^3 2q_0} \frac{e_q^2 \pi R^2}{2p^-} \frac{2\alpha_{\mathrm{em}}}{3k^2} \langle \mathrm{tr}(L^\dagger L) \rangle_{\mathrm{spin}}
$$

$$
\times 2\pi \delta(q^- + k^- - p^-) C(\mathbf{p}_\perp - \mathbf{q}_\perp - \mathbf{k}_\perp), \quad (11)
$$

where we define again

$$
C(\mathbf{l}_\perp) \equiv \int d^2 \mathbf{x}_\perp e^{i\mathbf{l}_\perp \cdot \mathbf{x}_\perp} \langle U(0) U^\dagger(\mathbf{x}_\perp) \rangle_\rho. \quad (12)
$$

Like in the case of real photon production, all the information about the nature of the medium crossed by the quark (in particular, all the dependence on the saturation scale Q_s) is contained in this function C.

At this point, it is useful to introduce the longitudinal momentum fraction of the virtual photon $z \equiv k^- / p^-$, as well as the total transverse momentum transfer between the nucleus and the quark $\mathbf{l}_\perp \equiv \mathbf{q}_\perp + \mathbf{k}_\perp$. The phase space d^4k of the lepton pair can be rewritten as $d^4k = \frac{1}{2} d(M^2) \times (dz/z) d^2 \mathbf{k}_\perp$, while the phase space of the outgoing quark can be written as $d^3 \mathbf{q}/(2\pi)^3 2q_0 = \frac{1}{2}(dq^-/q^-) \theta(q^-) d^2 \mathbf{l}_\perp$ [implicitly, $q^+ = \mathbf{q}_\perp^2/(2q^-)$]. In terms of these new variables, the inclusive differential cross section reads (for unit electric charge of quark)

$$
\frac{1}{\pi R^2} \frac{d\sigma_{\mathrm{incl}}^{q \, A \to q \, l^+ l^- \, X}}{dz \, d^2 \mathbf{k}_\perp \, d\log M^2}
$$

$$
= \frac{2\alpha_{\mathrm{em}}^2}{3\pi} \frac{d^2 \mathbf{l}_\perp}{(2\pi)^4} C(\mathbf{l}_\perp) \left\{ \left[\frac{1 + (1-z)^2}{z} \right] \right.
$$

$$
\times \frac{z^2 \mathbf{l}_\perp^2}{[\mathbf{k}_\perp^2 + M^2(1-z)][(\mathbf{k}_\perp - z\mathbf{l}_\perp)^2 + M^2(1-z)]}
$$

$$
- z(1-z) M^2 \left[\frac{1}{[\mathbf{k}_\perp^2 + M^2(1-z)]} \right.
$$

$$
\left. \left. - \frac{1}{[(\mathbf{k}_\perp - z\mathbf{l}_\perp)^2 + M^2(1-z)]} \right]^2 \right\}. \quad (13)
$$

This is our main result. It gives the differential cross section for inclusive production of dileptons in high energy quark-nucleus collisions and includes all the high gluon density effects in the nucleus. All the information about the high gluon density effects in the nucleus is contained in the function $C(\mathbf{l}_\perp)$ [9,10]. This function behaves as $1/l_\perp^4$ in the $l_\perp \gg Q_s$ (perturbative) region and like $1/l_\perp^2$ at $l_\perp \sim Q_s$. For $l_\perp \ll Q_s$, it is almost flat. Furthermore, the value of $l_\perp$ where the slope of the cross section changes strongly depends on rapidity. This slow down happens at higher values of $l_\perp$ in the forward rapidity region.

This expression reduces to the one found in [9] for real photon production if we take the limit $M^2 \to 0$ as it must. The main difference compared to the production of a real photon is the fact that the collinear singularities at $\mathbf{k}_\perp = z\mathbf{l}_\perp$ and $\mathbf{k}_\perp = 0$ are now screened by the invariant mass squared of the lepton pair, via the term $M^2(1-z) > 0$.

In order to relate Eq. (13) to proton-nucleus collisions, we will need to convolute Eq. (13) with the quark distribution function in a proton using collinear factorization theorem. Explicitly,

$$\frac{d\sigma_{\rm incl}^{p\,A\rightarrow q\,l^+l^-\,X}}{dz\,d^2\mathbf{k}_\perp\,d\log M^2}\sim\int dx\,q(x,Q_f^2)\frac{d\sigma_{\rm incl}^{q\,A\rightarrow q\,l^+l^-\,X}}{dz\,d^2\mathbf{k}_\perp\,d\log M^2}.$$

(14)

Furthermore, one will need to convolute the above cross section with a quark-hadron or quark-jet fragmentation function if one is interested in measuring both the outgoing hadron-jet as well as the dilepton. Otherwise, one can do the $l_\perp$ integration above to get the $pA\rightarrow l^+l^-X$ differential cross section.

Experimentally, one will be able to study M^2, $k_\perp^2$ and rapidity (z) dependence of the dilepton production cross section in $p-A$ collisions at RHIC in the near future. Here, we outline our qualitative predictions from the color glass condensate picture of a nucleus at high energy which will be straightforward to verify or falsify at RHIC.

First, as compared to the standard leading twist perturbative QCD, we expect that the partonic level cross section $d\sigma/dy\,d^2l_\perp$ will change its behavior from $1/l_\perp^4$ to $1/l_\perp^2$ for $l_\perp\sim Q_s$ and an even flatter behavior at smaller $l_\perp$, at fixed rapidity. Convoluting the partonic cross section with parton structure functions in order to get the proton-nucleus cross section will change the power of $l_\perp$. Nevertheless, we expect the difference in the power of $l_\perp$ to be observable even after the convolution [13].

Second, the change of the slope of the cross section from $1/l_\perp^4$ to $1/l_\perp^2$ will happen at a higher transverse momentum in the forward rapidity region than the midrapidity region. Indeed, the saturation scale of the nucleus near the fragmentation region of the proton is much larger than the value $Q_s^2\sim1-2$ GeV^2 usually quoted at midrapidity [14]. The growth of the saturation scale with energy is known from DIS experiments at the DESY ep collider HERA [5] and heavy ion collisions at RHIC [14].

For the same reason as above, transverse momentum broadening of the jet+dilepton system will depend on its rapidity: it will be larger at forward rapidities. This broadening proportional to Q_s adds up to the broadening due to initial "intrinsic transverse momentum" of the incoming quark. This effect has been neglected in our final result by setting $\mathbf{p}_\perp=0$. All it would take to keep both effects simultaneously would be to keep $\mathbf{p}_\perp\neq0$ in the calculation.

A more quantitative investigation of our results is beyond the scope of this work and will be pursued elsewhere. Nevertheless, we would like to point out that inclusion of the standard leading order perturbative QCD (PQCD) diagrams [16] such as dilepton production via quark-antiquark annihilation[2] and from direct (virtual) photon diagrams will be required for numerical accuracy. Since these diagrams are not affected by the strong classical field of the nucleus and do not interfere with the diagrams considered in this work, one can just add their contribution to our results. This way, one will have the full leading order (LO) $[O(\alpha_{em}^2)]$ and next LO (NLO) $[O(\alpha_s\,\alpha_{em}^2]$ dilepton production cross section in $p-A$ including the high gluon density effects in the nucleus [15].

We would like to emphasize that our result (13) can also be used for heavy ion collisions in the very forward rapidity region where valence quarks are the dominant partons in the projectile nucleus. The only difference with $p-A$ is that one would then need to convolute our cross section with the quark distribution function in a nucleus rather than a proton. This may make it possible to extract the shadowing function for quarks (at large x) in the projectile nucleus by considering the ratio of dilepton cross sections in $A-A$ and $p-A$ collisions at RHIC or the CERN Large Hadron Collider (LHC).

----

[2]In principle, one will have to include the effects of high gluon densities on sea quarks. However, this will have another factor of α_s and therefore is higher order.

[1] L.N. Lipatov, Sov. J. Nucl. Phys. **23**, 338 (1976); E.A. Kuraev, L.N. Lipatov, and V.S. Fadin, Sov. Phys. JETP **45**, 199 (1977); I. Balitsky and L.N. Lipatov, Sov. J. Nucl. Phys. **28**, 822 (1978).

[2] L.V. Gribov, E.M. Levin, and M.G. Ryskin, Phys. Rep. **100**, 1 (1983); A.H. Mueller and J.-W. Qiu, Nucl. Phys. **B268**, 427 (1986).

[3] L. McLerran and R. Venugopalan, Phys. Rev. D **49**, 2233 (1994); **49**, 3352 (1994); **50**, 2225 (1994).

[4] A. Ayala, J. Jalilian-Marian, L. McLerran, and R. Venugopalan, Phys. Rev. D **52**, 2935 (1995); **53**, 458 (1996); J. Jalilian-Marian, A. Kovner, L. McLerran, and H. Weigert, *ibid.* **55**, 5414 (1997); **59**, 014014 (1999); **59**, 034007 (1999); J. Jalilian-Marian, A. Kovner, and H. Weigert, *ibid.* **59**, 014015 (1999); A. Kovner and G. Milhano, *ibid.* **61**, 014012 (2000); A. Kovner, G. Milhano, and H. Weigert, *ibid.* **62**, 114005 (2000);

I. Balitsky, Nucl. Phys. **B463**, 99 (1996); Y. Kovchegov, Phys. Rev. D **61**, 074018 (2000); **54**, 5463 (1996); **55**, 5445 (1997); E. Iancu, A. Leonidov, and L. McLerran, Nucl. Phys. **A692**, 583 (2001); Phys. Lett. B **510**, 133 (2001); hep-ph/0202270; E. Ferreiro, E. Iancu, A. Leonidov, and L. McLerran, Nucl. Phys. **A703**, 489 (2002).

[5] K. Golec-Biernat and M. Wusthoff, Phys. Rev. D **59**, 014017 (1999); **60**, 114023 (1999); Eur. Phys. J. C **20**, 313 (2001).

[6] A. Kovner, L. McLerran, and H. Weigert, Phys. Rev. D **52**, 3809 (1995); **52**, 6231 (1995); Y. Kovchegov and D. Rischke, Phys. Rev. C **56**, 1084 (1997); A. Krasnitz and R. Venugopalan, Phys. Rev. Lett. **84**, 4309 (2000); **86**, 1717 (2001); D. Kharzeev and M. Nardi, Phys. Lett. B **507**, 121 (2001); D. Kharzeev and E. Levin, *ibid.* **523**, 79 (2001).

[7] R. Baier, A.H. Mueller, D. Schiff, and D. Son, Phys. Lett. B **539**, 46 (2002).

[8] A. Dumitru and J. Jalilian-Marian, Phys. Rev. Lett. **89**, 022301 (2002); Phys. Lett. B **547**, 15 (2002).

[9] F. Gelis and J. Jalilian-Marian, Phys. Rev. D **66**, 014021 (2002).

[10] F. Gelis and A. Peshier, Nucl. Phys. **A697**, 879 (2002); **A707**, 175 (2002).

[11] E. Berger, L. Gordon, and M. Klasen, Phys. Rev. D **58**, 074012 (1998); J.-C. Peng, hep-ph/9912371.

[12] C. Itzykson and J. B. Zuber, *Quantum Field Theory* (McGraw-Hill, New York, 1980).

[13] J. Lenaghan and K. Tuominen, hep-ph/0208007.

[14] D. Kharzeev, E. Levin, and M. Nardi, hep-ph/0111315.

[15] K.J. Eskola, V.J. Kolhinen, and C.A. Salgado, Eur. Phys. J. C **9**, 61 (1999).

[16] R.K. Ellis, W.J. Stirling, and B.R. Weber, *QCD and Collider Physics* (Cambridge University Press, Cambridge, England, 1996).